

## Dominance of Phonon Friction for a Xenon Film on a Silver (111) Surface

M. S. Tomassone, J. B. Sokoloff, A. Widom, and J. Krim

*Department of Physics and Center for Interdisciplinary Research on Complex Systems,  
Northeastern University, Boston, Massachusetts 02115*

(Received 21 November 1996)

Molecular dynamic simulations for a Xe film sliding on an Ag(111) substrate are performed from the submonolayer through the bilayer regime, which, when compared to both friction and surface resistivity measurements, demonstrate that the friction in this system is dominated by phonon excitations. Slip times are found both by direct calculation of the decay of the center-of-mass velocity, as well as from the decay of the velocity correlation function. Agreement of the slip times from the two methods supports the occurrence of a friction force linear in velocity over a wide velocity range. [S0031-9007(97)04756-X]

PACS numbers: 46.30.Pa

Although tribology, the study of friction and wear, has been of technological interest since ancient times [1,2], the topic continues to rouse interest today [3–12]. Rapid progress in experimental, theoretical, and computational methods provides new insights into the atomic origins of frictional energy dissipation. When a thin film slides on a metal substrate there exists dissipation of energy via two mechanisms: (i) electronic excitations in the metallic substrate [4,9], and (ii) phonon excitations in the film or in the substrate [10]. The dissipation of energy can be characterized by the slip time  $\tau$  (i.e., the time it takes for the film's speed to fall to  $1/e$  of its original value, assuming it is stopped by friction) or equivalently by a damping coefficient  $\eta \sim 1/\tau$ .

In this Letter we study the phonon contribution to friction for Xe films sliding along an Ag(111) substrate using molecular dynamics simulations. It is of great interest to determine the relative contributions of the phonons and electrons to friction, since to date it is not clear which is dominant. To this end, we compare our results with the slip time versus coverage data reported by Daly and Krim [6], and with the electrical resistivity versus coverage data of Dayo and Krim [7]. The results of this comparison provide convincing evidence that phonon excitations make a dominant contribution to the friction for this system.

We determine the slip time as a function of coverage, defined as the number of atoms in the film per unit area. We treat a range of film coverages, from submonolayer to bilayer. The slip time is determined by two methods. In the first method, an initial center-of-mass velocity  $\mathbf{V}_0$  is produced by an external force exerted on the film for  $t < 0$ . The external force is turned off for  $t > 0$ , and  $\tau$  is determined by the resulting velocity decay  $\mathbf{V}_0 e^{-t/\tau}$ . In the second method, no external force is applied. The slip time is determined by the behavior of the thermal equilibrium autocorrelation for the center-of-mass velocity as a function of time. The autocorrelation function is related to the linear response of the system to a small perturbation by the fluctuation-dissipation theorem [12,13], which holds in the

limit of zero applied force and, hence, zero velocity. This method is the only one which is valid at the 1 cm/s velocities appropriate for experiments using the quartz crystal microbalance (QCM) [6,8]; all other molecular dynamics methods for determining the slip time are only valid for velocities of the order of  $10^3$  cm/s or more.

Molecular dynamics simulations of sliding friction have traditionally employed *thermostats* which add or remove energy to or from the system in order to achieve constant temperature. Thermostats used in molecular dynamics have the side effect of damping the atomic motions, resulting in an additional contribution to friction [10,11]. In order to study friction in a situation free of such complications, we employ a thermostat solely to establish statistical thermal equilibrium, but then turn it off while monitoring the system's properties. The absence of a thermostat in the simulation allows us to focus exclusively on the film's dissipation due to phonons.

The model Hamiltonian for  $N$  film atoms of mass  $m$  at positions  $\mathbf{r}_k$  ( $k = 1, \dots, N$ ) is given by

$$H \equiv \sum_{k=1}^N \frac{\mathbf{p}_k^2}{2m} + U(\mathbf{r}_1, \dots, \mathbf{r}_N), \quad (1)$$

where  $\mathbf{p}_k$  is the momentum of the atom  $k$ , and the total potential  $U(\mathbf{r}_1, \dots, \mathbf{r}_N)$  is given by

$$U(\mathbf{r}_1, \dots, \mathbf{r}_N) \equiv \sum_{k=1}^N U_s(\mathbf{r}_k) + \sum_{j < k=1}^N V(|\mathbf{r}_j - \mathbf{r}_k|). \quad (2)$$

Here,  $U_s(\mathbf{r}_k)$  is a single particle potential describing the interaction between the  $k$ th film atom and the substrate, and  $V(|\mathbf{r}_j - \mathbf{r}_k|)$  is the pair potential interaction between the  $j$ th and  $k$ th atoms in the film.

The interaction between two Xe atoms is given by a Lennard-Jones potential

$$V(r) = 4\varepsilon \left[ \left( \frac{\sigma}{r} \right)^{12} - \left( \frac{\sigma}{r} \right)^6 \right], \quad (3)$$

where  $\varepsilon = 19.83$  meV, and  $\sigma = 4.055$  Å [14]. The interaction between a Xe atom and the substrate can be

described by a substrate potential without internal degrees of freedom given by [15]

$$U_s(\mathbf{r}_{\parallel}, z) = U_0(z) + U_1(z) \sum_{\{\mathbf{G}\}} \cos(\mathbf{G} \cdot \mathbf{r}_{\parallel}), \quad (4)$$

where  $\mathbf{r}_{\parallel} = (x, y)$  are the coordinates of the Xe atom parallel to the substrate, and  $\{\mathbf{G}\}$  is the set of the six shortest reciprocal lattice vectors of the substrate. The first term in Eq. (4) describes the mean interaction of the atoms with the substrate, and the second term describes the periodic corrugation potential.

Expressions for  $U_0(z)$  and  $U_1(z)$  were derived by Steele [15], assuming that the substrate potential  $U_s(\mathbf{r})$  is a sum of Lennard-Jones potentials between one film atom and all of the atoms in the substrate. However, a potential such as  $U_s(\mathbf{r})$ , which is a sum of Lennard-Jones potentials, is not a correct description of the interaction of a metallic surface with a noble gas atom. The corrugation potential is reduced (from the value found by summing Lennard-Jones potentials) due to electronic screening. For this reason we employ a weaker corrugation potential, as did Cieplak *et al.* in Ref. [10]. The corrugation potential we use is

$$U_1(z^*) = \alpha e^{-g_1 z^*} \sqrt{\frac{\pi}{2g_1 z^*}} \left[ \frac{A^{*6}}{30} \left( \frac{g_1}{2z^*} \right)^5 - 2 \left( \frac{g_1}{2z^*} \right)^2 \right], \quad (5)$$

where  $\alpha = 4\pi \epsilon_{\text{Xe/Ag}} A^{*6} / \sqrt{3}$ ,  $z^* = z/a$ ,  $a = 2.892 \text{ \AA}$  is the lattice constant of the substrate,  $A^* = \sigma_{\text{Xe/Ag}}/a$ ,  $g_1 = 4\pi/\sqrt{3}$ . We calculate the Lennard-Jones parameters  $\sigma_{\text{Xe/Ag}}$  and  $\epsilon_{\text{Xe/Ag}}$  by fitting (i) the position of the minimum of  $U_0(z)$  to the distance between a Xe atom in the first layer and the ion cores of the substrate ( $z_0$ ), and (ii) the attractive well depth to the binding energy of one Xe atom to the Ag substrate ( $U_0(z_0) = -211 \text{ meV}$ , from [16]). We find  $\sigma_{\text{Xe/Ag}} = 4.463 \text{ \AA}$  and  $\epsilon_{\text{Xe/Ag}} = 13.88 \text{ meV}$ .

The corrugation potential  $U_1(z)$  in Eq. (5) falls off exponentially at large  $z$ . The above parameters give  $U_1(z_0^*) \sum_{\{\mathbf{G}\}} \cos(\mathbf{G} \cdot \mathbf{r}_{\parallel}) = 2.7 \text{ meV}$  (for the maximum value of this sum), in contrast to the corresponding value of  $10.13 \text{ meV}$  for Steele's potential at  $z_0$  [15]. Our corrugation gives good agreement with the experimental value of the slip time.

Our simulations are carried out at an equilibrium temperature of  $T = 77.4 \text{ K}$ , and the particles move in a three dimensional box of size  $20a \times 10a\sqrt{3} \times 10\sigma$ . The time scale for vibrations of the adsorbed film atoms is  $t_0 = \sqrt{(m\sigma^2/\epsilon)} = 3.345 \text{ ps}$ , with  $m = 2.16 \times 10^{-22} \text{ g}$ . Periodic boundary conditions in the  $x$  and  $y$  directions are employed along with a hard wall boundary condition in the  $z$  direction at the top of the box.

We change the coverage by changing the number of Xe atoms  $N$ . We use  $60 \leq N \leq 370$ . All atoms are initially in the gas phase. The atoms condensed in  $250t_0$  or less and formed a triangular lattice incommensurate with the substrate fcc(111) surface. A thermostat is used only to

establish thermal equilibrium. To calculate the slip time we use two methods:

Method I: An external force (parallel to the substrate surface) is applied to all film particles for approximately  $100t_0$ . The external force is then removed. This induces an initial center-of-mass velocity  $\mathbf{V}_0$  in the film which decays at later times as  $\mathbf{V}_0 e^{-t/\tau}$ . Indeed, we find an exponential decay as shown in Fig. 1. The slip time versus coverage results obtained in this manner are shown in Fig. 2(a). The thermostat is turned off while the decay of the center-of-mass velocity takes place, and the temperature rises by, at most,  $13 \text{ K}$  during this process, which occurs for the largest value for the initial velocities that we use in these calculations ( $0.6\sigma/t_0$ ).

Method II: In this method no external force is applied at any time. In experiments using QCM [8], one conventionally describes the data by the linear response in the force per unit area  $\delta f$  to an applied substrate velocity  $\delta V$  at complex frequency  $\zeta$ . This response defines the acoustic impedance of the film,  $Z(\zeta) \equiv \lim_{\delta f \rightarrow 0} (\delta f / \delta V)$ . The Kubo formula for the acoustic impedance has been derived [12] to be

$$Z(\zeta) = -i\zeta\rho_2 \left( 1 + i\zeta \int_0^\infty C(t) e^{i\zeta t} dt \right), \quad (6)$$

where  $\rho_2 \equiv Nm/A$  is the film mass per unit area  $A$ , and the thermal equilibrium autocorrelation function

$$C(t - t') \equiv \frac{\langle V_x(t) V_x(t') \rangle}{\langle V_x(0)^2 \rangle}. \quad (7)$$

In Eq. (7),  $V_x(t)$  is the center-of-mass velocity of the film in the  $x$  direction [17]. The slip time model [12] may be written as a Drude-Darcy law impedance  $Z(\zeta) = -i(\zeta\rho_2)/(1 - i\zeta\tau)$  or, equivalently, as the autocorrelation function

$$C(t - t') = \exp\left(-\frac{|t - t'|}{\tau}\right). \quad (8)$$

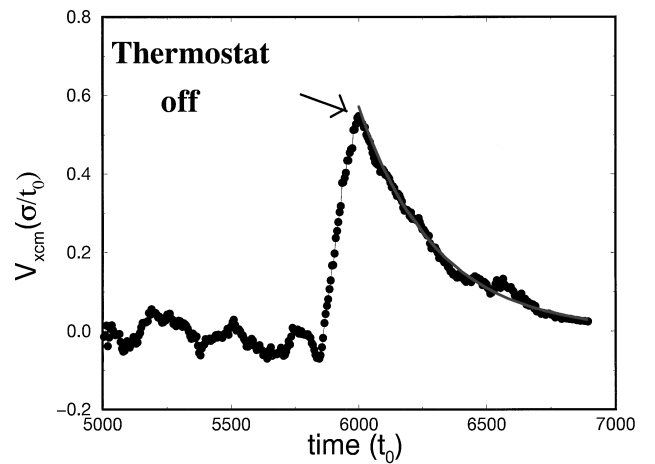


FIG. 1. Typical decay of the center-of-mass velocity (in units of  $\sigma/t_0$ ) after applying the external force. After the force and thermostat are turned off, the velocity decays; and this portion of the graph is fitted to an exponential curve as predicted by the linear friction force law to obtain the slip time (method I).

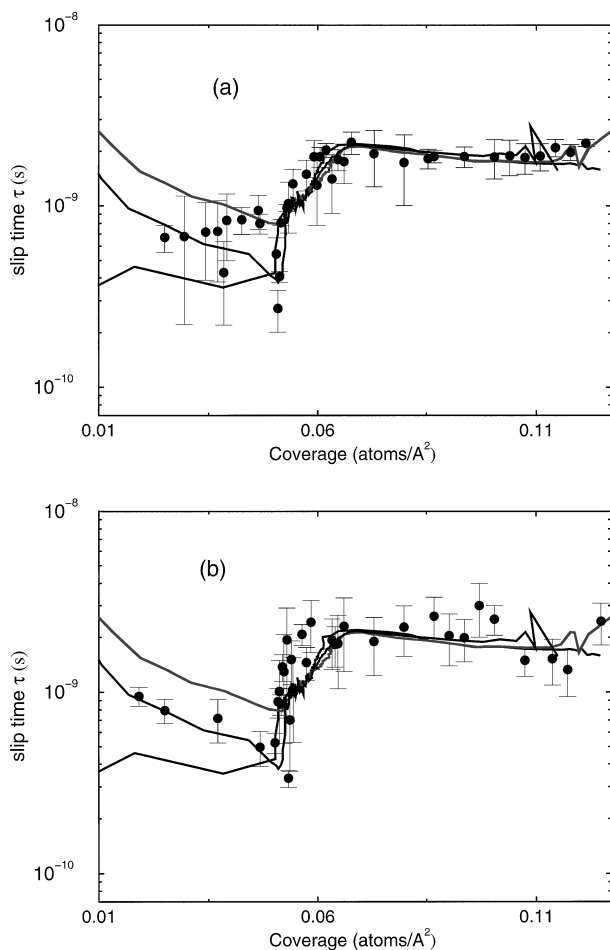


FIG. 2. Slip time  $\tau$  (in units of sec) versus coverage (in units of number of particles per  $\text{\AA}^2$ ) for the two methods used; (a) method I, (b) method II. Solid lines in both figures are three of the experimental curves from Ref. [6], included for comparison. There is semiquantitative agreement with experiment. Both methods reach a minimum near  $0.0563 \text{ atom}/\text{\AA}^2$ .

Equation (8) is the basis of the second method for calculating  $\tau$ . The thermal average in Eq. (7) is replaced by a time average over a time  $t_{\text{tot}}$

$$\langle V_x(t)V_x(t') \rangle = \frac{1}{t_{\text{tot}}} \int_0^{t_{\text{tot}}} V_x(t+s)V_x(t'+s)ds. \quad (9)$$

In Fig. 2(b), the values of the slip time as a function of film coverage found using method II are shown. Methods I and II yield results which are qualitatively similar to each other and to previous experimental results, as can be seen by comparing Figs. 2(a) and 2(b).

We find a dip in the slip time near a coverage of  $0.0563 \text{ atom}/\text{\AA}^2$  followed by a sharp rise. The minimum in  $\tau$  corresponds to the uncompressed monolayer (see Fig. 2). [Slight differences in the positions of these features in Figs. 2(a) and 2(b) are likely to be due to the heating that occurs in method I.] We are able to observe directly, in the simulations, a compression of the monolayer when the coverage varies from  $0.0563 \text{ atom}/\text{\AA}^2$  to  $0.0594 \text{ atom}/\text{\AA}^2$ . The average interparticle spacings at

these two coverages are, respectively,  $4.53 \text{ \AA}$  and  $4.4 \text{ \AA}$ . These values are very close to those reported experimentally by Unguris *et al.* [19] ( $4.52 \text{ \AA}$  and  $4.39 \text{ \AA}$  for the uncompressed and fully compressed monolayer). The fact that our simulations, which include only the phonon contribution to friction, reproduce the experimental results provides strong evidence that phonon friction dominates in the system under study. Furthermore, the fact that the electrical resistivity does not reveal any coverage dependence (reminiscent of the observed structure in the experimental slip time versus coverage curve) [7] gives further support to this conclusion.

The structure factor,

$$S(\mathbf{Q}) \equiv \frac{1}{N} \left\langle \sum_{i,j}^N \cos[\mathbf{Q} \cdot (\mathbf{r}_i - \mathbf{r}_j)] \right\rangle, \quad (10)$$

has also been calculated. In Fig. 3 we show the Bragg peaks in the  $\mathbf{Q} = (Q_x, Q_y, 0)$  plane for three different coverages, corresponding to the submonolayer, slightly below the uncompressed monolayer and the compressed monolayer coverages. The Bragg peaks for the larger slip times (compressed monolayer) are sharper than the Bragg peaks for the smaller slip times (submonolayer and slightly uncompressed monolayer). Thus, the lattices corresponding to small slip times have more disorder than lattices with large slip times. The tilting of the Bragg peaks shown in Figs. 3(a) and 3(c) is likely to be due to rotational epitaxy [20]. The fact that it does not occur for Fig. 3(b) is likely to be related to our use of periodic boundary conditions. A more detailed discussion of this phenomenon will be reserved for further publications.

Persson and Nitzan [11] have recently calculated friction for the present system using molecular dynamics in a model that includes a Langevin thermostat, which they identify with the effect of electronic excitations in the substrate. This thermostat uses unequal damping constants in directions parallel and perpendicular to the sliding direction (i.e.,  $\eta_{\parallel} = 6.2 \times 10^8 \text{ sec}^{-1}$  taken to represent electron friction and  $\eta_{\perp} = 2.5 \times 10^{11} \text{ sec}^{-1}$ ). They find a resulting friction constant  $\eta_{\text{tot}} \approx 6.32 \times 10^8 \text{ sec}^{-1}$  in their simulations, for a coverage slightly below a monolayer. Assuming  $\eta_{\text{tot}} = \eta_{\parallel} + \eta_{\text{phon}}$ , they find that the phonon contribution to friction  $\eta_{\text{phon}}/\eta_{\text{tot}} = 0.02$ . We have performed simulations using the substrate potential of Eqs. (4) and (5) with the same Langevin thermostat and damping constants as Persson and Nitzan. We find  $\eta_{\text{tot}} = 2.45 \times 10^9 \text{ sec}^{-1}$ , so that  $\eta_{\text{phon}}/\eta_{\text{tot}} = 0.75$ . Thus, even if we include the value of  $\eta_{\parallel}$  used by Persson and Nitzan, phonon friction dominates, which is consistent with our previous conclusion.

In conclusion, we perform molecular dynamics simulations of Xe/Ag(111) in a thermostat-free environment. We are able to semiquantitatively reproduce the experimental data [6] by means of two independent methods which simulate sliding speeds at least 3 orders of magnitude apart. In particular, our simulation reproduces the

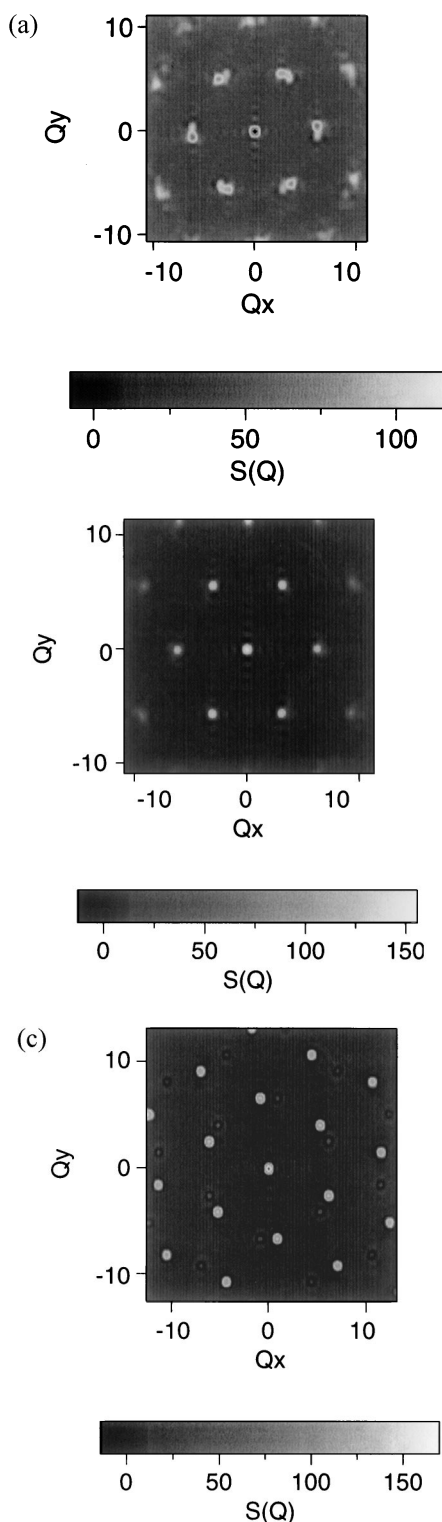


FIG. 3. Bragg peaks for (a) a submonolayer coverage,  $0.040 \text{ atom}/\text{\AA}^2$ , (b) slightly below the uncompressed monolayer coverage,  $0.0538 \text{ atom}/\text{\AA}^2$ , and (c) the compressed monolayer coverage,  $0.0594 \text{ atom}/\text{\AA}^2$ .

distinctive dip in the submonolayer regime found in experiment. This result, combined with the fact that the electrical surface resistivity is found to be nearly constant

in this regime [7] suggests that the phonon contribution dominates over the electron contribution for this system. The fact that the simulations yield comparable slip times for greatly varying sliding speeds demonstrates the linearity in velocity of the friction governing this system.

This work has been supported in part by NSF Grant No. DMR9204022 and by a U.S. Department of Energy Grant No. DE-FG02-96ER45585. We would like to thank Professor H.E. Stanley for his aid. One of us (M.S.T.) would like to thank H.A. Makse for useful discussions.

- 
- [1] F.P. Bowden and D. Tabor, *Friction and Lubrication* (Methuen, London, 1967); J.F. Archard, Proc. R. Soc. London A **243**, 190 (1957).
  - [2] D. Dowson, *History of Tribology* (Longman, London, 1979).
  - [3] J.B. Sokoloff, Phys. Rev. B **42**, 760 (1990); Phys. Rev. B **42**, 6745(E) (1990); Phys. Rev. B **47**, 6106 (1993); Wear **167**, 59 (1993); Phys. Rev. Lett. **71**, 3450 (1993); Phys. Rev. B **51**, 15 573 (1995).
  - [4] J.B. Sokoloff, Phys. Rev. B **52**, 5318 (1995).
  - [5] E.T. Watts, J. Krim, and A. Widom, Phys. Rev. B **41**, 3466 (1990); A. Widom and J. Krim, Phys. Rev. E **49**, 4154 (1994).
  - [6] C. Daly and J. Krim, Phys. Rev. Lett. **76**, 803 (1996).
  - [7] A. Dayo and J. Krim, in *Friction, Arching, Contact Dynamics*, edited by D.E. Wolf and P. Grassberger (World Scientific, Singapore, 1997) p. 47.
  - [8] J. Krim, D.H. Solina, and R. Chiarello, Phys. Rev. Lett. **66**, 181 (1991); J. Krim, Comments Condensed Matter Phys. **17**, 263 (1995).
  - [9] B.N.J. Persson and A.I. Volokitin, J. Chem. Phys. **103**, 8679 (1995).
  - [10] M. Cieplak, E.D. Smith, and M.O. Robbins, Science **265**, 1209 (1994); Phys. Rev. B **54**, 8252 (1996).
  - [11] B.N.J. Persson and A. Nitzan, Surf. Sci. **367**, 261 (1996).
  - [12] J. Krim and A. Widom, Phys. Rev. B **38**, 12 184 (1988).
  - [13] R. Kubo, M. Toda, and N. Hashitsume, *Statistical Physics II: Nonequilibrium Statistical Mechanics* (Springer-Verlag, Heidelberg, 1995), 2nd ed.
  - [14] J.G. Dash, *Films of Solid Surfaces* (Academic Press, London, 1975).
  - [15] W. Steele, Surf. Sci. **36**, 317 (1973).
  - [16] G. Vidali, G. Ihm, H. Y. Kim, and M. Cole, Surf. Sci. Rep. **12**, 133 (1991).
  - [17] In our simulations we take  $V_x$  as the center-of-mass velocity minus its mean  $\langle V_x \rangle$ . Subtracting the mean center-of-mass velocity is a standard technique that, in a molecular dynamics simulation, ensures that the correlation goes to zero at long times [18].
  - [18] J.M. Haile, *Molecular Dynamics Simulation: Elementary Methods* (Wiley, New York, 1992).
  - [19] J. Unguris, W.L. Bruch, E.R. Moog, and M.B. Webb, Surf. Sci. **87**, 415 (1979).
  - [20] A.D. Novaco and J.P. McTague, Phys. Rev. Lett. **38**, 1286 (1977); Phys. Rev. B **19**, 5299 (1979).